NASA/CR–20220001824

Further Development of a Function Generator Technique

Michael S. Woronowicz
KBR, Inc., Greenbelt, Maryland
Goddard Space Flight Center, Greenbelt, Maryland

March 2022

NASA STI Program ... in Profile

Since its founding, NASA has been dedicated to the advancement of aeronautics and space science. The NASA scientific and technical information (STI) program plays a key part in helping NASA maintain this important role.

The NASA STI program operates under the auspices of the Agency Chief Information Officer. It collects, organizes, provides for archiving, and disseminates NASA's STI. The NASA STI program provides access to the NTRS Registered and its public interface, the NASA Technical Reports Server, thus providing one of the largest collections of aeronautical and space science STI in the world. Results are published in both non-NASA channels and by NASA in the NASA STI Report Series, which includes the following report types:

- TECHNICAL PUBLICATION. Reports of completed research or a major significant phase of research that present the results of NASA Programs and include extensive data or theoretical analysis. Includes compilations of significant scientific and technical data and information deemed to be of continuing reference value. NASA counterpart of peer-reviewed formal professional papers but has less stringent limitations on manuscript length and extent of graphic presentations.

- TECHNICAL MEMORANDUM. Scientific and technical findings that are preliminary or of specialized interest, e.g., quick release reports, working papers, and bibliographies that contain minimal annotation. Does not contain extensive analysis.

- CONTRACTOR REPORT. Scientific and technical findings by NASA-sponsored contractors and grantees.

- CONFERENCE PUBLICATION. Collected papers from scientific and technical conferences, symposia, seminars, or other meetings sponsored or co-sponsored by NASA.

- SPECIAL PUBLICATION. Scientific, technical, or historical information from NASA programs, projects, and missions, often concerned with subjects having substantial public interest.

- TECHNICAL TRANSLATION. English-language translations of foreign scientific and technical material pertinent to NASA's mission.

Specialized services also include organizing and publishing research results, distributing specialized research announcements and feeds, providing information desk and personal search support, and enabling data exchange services.

For more information about the NASA STI program, see the following:

- Access the NASA STI program home page at http://www.sti.nasa.gov

- E-mail your question to help@sti.nasa.gov

- Phone the NASA STI Information Desk at 757-864-9658

- Write to:
  NASA STI Information Desk
  Mail Stop 148
  NASA Langley Research Center
  Hampton, VA 23681-2199

NASA/CR–20220001824

Further Development of a Function Generator Technique

Michael S. Woronowicz
KBR, Inc., Greenbelt, Maryland
Goddard Space Flight Center, Greenbelt, Maryland

National Aeronautics and
Space Administration

Goddard Space Flight Center
Greenbelt, Maryland 20771-0001

March 2022

Acknowledgments

The author gratefully acknowledges support from NASA Contract NNG15CR64C, Eve Woodridge, Kristina Montt de Garcia, and Randy Hedgeland of GSFC Code 546, and Dong-Shiun Lin and Ray Levesque, KBR, Inc.

Level of Review: This material has been technically reviewed by technical management.

Available from

NASA STI Program Mail
Stop 148
NASA's Langley Research
Center Hampton, VA
23681-2199

National Technical Information Service
5285 Port Royal Road
Springfield, VA 22161
703-605-6000

This report is available in electronic form at

https://ntrs.nasa.gov

Abstract

Further features and properties of functions generated by generalization of the process originally uncovered to describe the evolution of pressure in a rigid volume due to outgassing or desorption are explored. Properties presented include development of a general Maclaurin series associated with these functions, a limitation in using integration by parts to produce asymptotic expansions, and a general description of an implicit Adams-Moulton method for numerical quadrature of transformed functions. These developments are then applied to develop and explore functions that solve the Sievert integral and the modified Bessel function of the first kind, order zero. Features of the error function and the incomplete lower gamma function are also considered.

Introduction

Investigation of an isothermal gas load differential equation developed from a general mass conservation statement was presented in Refs. 1 & 2 in support of satellite observatory program activities at NASA Goddard Space Flight Center. The evolution of pressure within a rigid, pumped volume under high vacuum due to theoretical, diffusion-limited outgassing from a source of essentially infinite thickness was described in terms of the Dawson function $D(x)$.[1,2] A more general solution was found for decaying sources following a power-law model upon discovery of a procedure that gave rise to a new function.[1,2] This process was subsequently used to generate other functions describing theoretical, diffusion-limited outgassing from a source having finite thickness and the transient intensity of column density due to a free expansion into high vacuum over a finite period.[2] Each of these new functions solves integrals that have may not have been previously reported.

Certain properties of functions generated by the technique described in Refs. 1 & 2 were noted. The purpose of this report is to present further observations associated with these properties and to apply them to explore the Sievert integral as well as existing functions defined by integration such as the modified Bessel function of the first kind, order zero, the error function used to describe diffusion processes, and the lower incomplete gamma function.

Analytical Development

If an integral having the general form

$$\int_0^s \frac{e^u}{f(u)} du \tag{1}$$

may be transformed to something proportional to the following via an appropriate variable substitution,

$$I(x) = \int e^{g(x)} dx, \tag{2}$$

the integral may be scaled to produce a function $F(x)$ in the transformed space produced by the variable substitution.

$$F(x) \equiv I(x) e^{-g(x)} = e^{-g(x)} \int e^{g(x)} dx. \tag{3}$$

Function $F(x)$ will satisfy its own differential equation:

$$\boxed{\frac{dF}{dx}+F\frac{dg}{dx}=1}. \tag{4}$$

Equation 4 may also be written as $F' + g'F = 1$.

Asymptotic Expansion

Working with Eq. (3), the terms of an asymptotic expansion may be obtained using integration by parts. Ignoring definite integration limits, it may be developed in this fashion:

$$\begin{aligned} I(x) &= \int e^{g(x)}dx = \int \frac{1}{g'}\frac{de^{g(x)}}{dx}dx = \frac{e^{g(x)}}{g'} - \int \left(\frac{1}{g'}\right)' \frac{1}{g'}\frac{de^{g(x)}}{dx}dx \\ &= \frac{e^{g(x)}}{g'} - \frac{e^{g(x)}}{g'}\left(\frac{1}{g'}\right)' + \int \left(\frac{1}{g'}\left(\frac{1}{g'}\right)'\right)' \frac{1}{g'}\frac{de^{g(x)}}{dx}dx = \dots . \end{aligned} \tag{5}$$

The general form for $F(x)$ becomes

$$F(x) \xrightarrow[x\to\infty]{} \frac{1}{g'} - \frac{1}{g'}\left(\frac{1}{g'}\right)' + \frac{1}{g'}\left(\frac{1}{g'}\left(\frac{1}{g'}\right)'\right)' - \frac{1}{g'}\left(\frac{1}{g'}\left(\frac{1}{g'}\left(\frac{1}{g'}\right)'\right)'\right)' + \dots \tag{6}$$

For this expression to be a valid asymptotic expansion for large x in nonperiodic functions, one must demonstrate that the remainder is much lower than the leading term, or that their ratio approaches zero as $x \to \infty$ so the expansion will converge. Often this can be approximated by showing that ratios of successive terms have the same behavior.

Example: Dawson Function

The Dawson function $D(x)$ was found to fit this scheme,[1,2] and will be used to compare results developed in this work to properties already identified in reference literature. By definition,[3,4]

$$D(x) \equiv e^{-x^2}\int_0^x e^{x^2}dx . \tag{7}$$

According to Eqns. (3) & (4), $g(x) = x^2$ and $D' + 2xD = 1$. Application of Eq. (6) indicates

$$D(x) \xrightarrow[x\to\infty]{} \frac{1}{2x} + \frac{1}{4x^3} + \frac{3}{8x^5} + \frac{15}{16x^7} + \frac{105}{32x^9} + \frac{945}{64x^{11}} + \dots = \sum_{k=0}^{\infty} \frac{(2k-1)!!}{2^{k+1}x^{2k+1}}. \tag{8}$$

With ratios of succeeding terms falling off as x^{-2}, this should describe $D(x)$ for large x, which it does. Eq. (8) agrees with large argument expansions for $D(x)$ found in the literature.[3,4] Function $D(x)$ along with its asymptotic expansion in Fig. 1 below.

Integration Limit Effect

The convenient development presented above does not account for the impact of the lower integration limit when definite integrals must be considered. The effect of integration by parts cannot be ignored in some instances when the lower limit produces a singularity. In Eq. (9) below, the integration interval is broken into two parts, where a represents a convenient constant value for the integral under consideration.

$$\begin{aligned} I(x) &= \int_0^x e^{g(x)}dx = \int_0^a e^{g(x)}dx + \int_a^x e^{g(x)}dx = \int_0^a e^{g(x)}dx + \int_a^x \frac{1}{g'}\frac{de^{g(x)}}{dx}dx \\ &= \int_0^a e^{g(x)}dx + \left[\frac{e^{g(x)}}{g'}\right]_a^x - \int_a^x \left(\frac{1}{g'}\right)' \frac{1}{g'}\frac{de^{g(x)}}{dx}dx \\ &= \boxed{\int_0^a e^{g(x)}dx - \frac{e^{g(a)}}{g'(a)}} + \frac{e^{g(x)}}{g'} - \int_a^x \left(\frac{1}{g'}\right)' \frac{1}{g'}\frac{de^{g(x)}}{dx}dx = \ldots . \end{aligned} \tag{9}$$

The first two terms in the last line of Eq. (9) represent a number. While it is assumed this number will be small compared to the expansion terms as x becomes large, sometimes this evaluation involves a singularity. There are some functions for which direct integration by parts fails to produce the correct asymptotic expansion, such as for the error function erf(x) and the lower incomplete gamma function $\gamma(s, x)$. It is noted that such functions tend to be produced by evaluating their complementary functions instead.

Critical Point Condition

The general condition for reaching a local maximum or minimum point for a function occurs when $F' = 0$. From Eq. (4):

$$F_{crit} = \frac{1}{g'}. \tag{10}$$

This expression also represents the first term in the general asymptotic expansion for $F(x)$, which means for cases where there is a valid asymptotic expansion that the first term will also intersect local extrema for finite argument if they are present in the transformed function as well.

A plot of the Dawson function along with an increasing number of terms in its asymptotic expansion is presented in Fig. 1. The first term intersects the function's maximum value of $D(x) = 0.54103$ at $x \approx 0.9241$.[4]

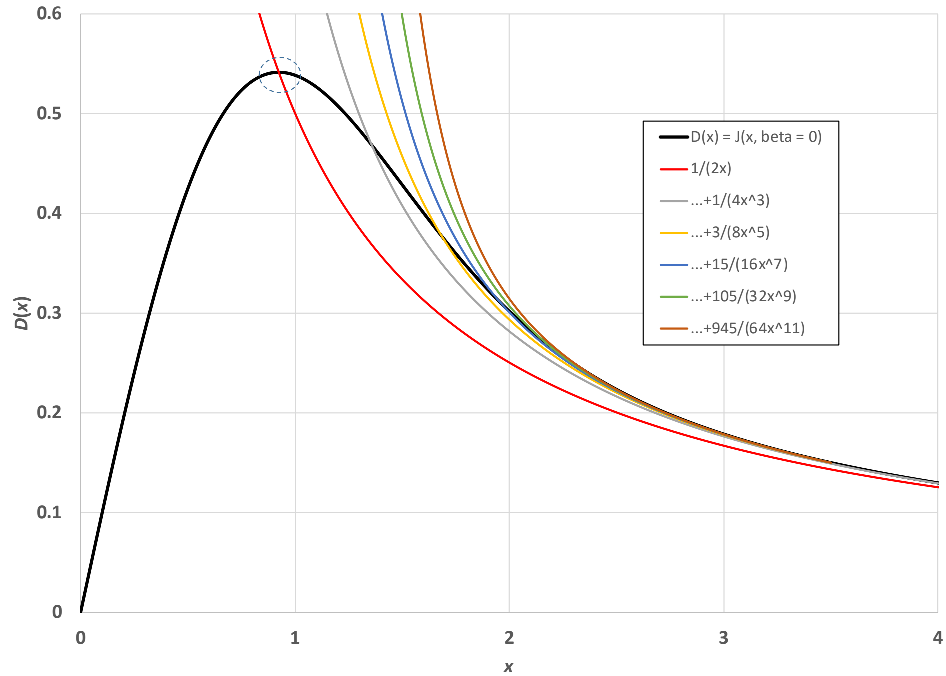

Figure 1. Dawson function $D(x)$, along with an increasing number of terms from its asymptotic expansion for large x.

Inflection Point Condition

Inflection points may be computed for these functions by setting their second derivative to zero. Starting with Eq. (4) to obtain an expression for F'':

$$\frac{d}{dx}\left(F' + g'F = 1\right) \rightarrow F'' + g''F + g'F' = 0\,. \tag{11}$$

But since *F'* + *g'F* = 1, substitution into Eq. (11) yields

$$F''(x) = \left[(g')^2 - g''\right]F - g'\,. \tag{12}$$

When F'' = 0, then

$$F_{\text{infl.pt.}} = \frac{g'}{\left[\,g'^{\,2} - g''\right]}\,. \tag{13}$$

Again, using the Dawson function as an example,

$$D(x)_{\text{infl.pt}} = \frac{x}{2x^2 - 1}\,. \tag{14}$$

Equation 14 produces this condition at (*x*, *D*) ≈ (1.502, 0.42768), as is accepted.[4] One comment for this function in particular is that since the terms of the asymptotic expansion are all positive, that series will not be able to conform to *D*(*x*) ahead of its inflection point (see Fig. 1).

Maclaurin Series

The Maclaurin series is a special case of the Taylor series expansion about *x* = 0:

$$f(x) = f(0) + x\,f'(0) + \frac{x^2}{2!}f''(0) + \frac{x^3}{3!}f'''(0) + \ldots + \frac{x^n}{n!}f^{(n)}(0) + \ldots \tag{15}$$

Maclaurin series terms for $F\ x$ may be computed by repeated application of taking derivatives of Eq. (4). In this case one may begin with Eq. (12) and substitute Eq. (4) where suitable to relate each derivative to *F* without derivatives. After some manipulation, one finds the transformed function may be expressed as

$$\begin{aligned} F(x) &= F(0) + x - \sum_{n=0}^{\infty} \frac{x^{n+1}}{(n+1)!}\frac{d^n}{dx^n}\left(g'F\right)\Big|_{x=0} \\ &= F(0) + x - \sum_{n=0}^{\infty} \frac{x^{n+1}}{(n+1)!}\sum_{k=0}^{n}\frac{n!}{(n-k)!\,k!}\,g^{(n-k+1)}(0)F^{(k)}(0). \end{aligned} \tag{16}$$

The ratio of factorials may be expressed in terms of binomial coefficients:

$$F(x) = F(0) + x - \sum_{n=0}^{\infty} \frac{x^{n+1}}{(n+1)!} \sum_{k=0}^{n} \begin{pmatrix} n \\ k \end{pmatrix} g^{(n-k+1)}(0) F^{(k)}(0). \tag{17}$$

Although not always true, often it appears *F*(0) = 0 and the limiting behavior for *F*(*x*) equates it to independent variable *x*. This characteristic linear dependence will be observed for several cases in upcoming sections.

Returning to the Dawson function, we may work with Eq. (17) to produce

$$D(x) = x - \frac{2}{3}x^3 + \frac{4}{15}x^5 - \frac{8}{105}x^7 + \dots. \tag{18}$$

Truncated series including the first terms of the Maclaurin series progression for the Dawson function are plotted along with *D*(*x*) in Fig. 2.

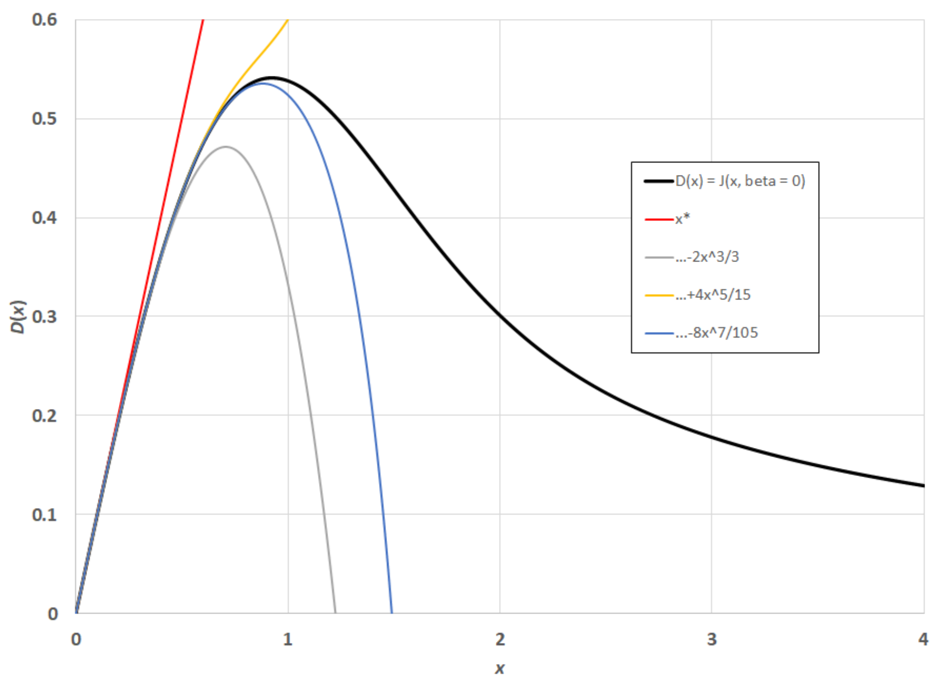

Figure 2. Dawson function *D*(*x*), along with an increasing number of terms from its Maclaurin series for small *x*.

Numerical Quadrature Scheme

One may generate the transformed function *F*(*x*) beginning from some minimum value for *x* (say zero) and assuming a value for $F(x_{min})$ (usually also choosing zero). It is also possible that $g'(0) = 0$, which may complicate matters or lead to errors for small *x*.

Stepping forward in increments of the independent variable *x* with interval $h \equiv \Delta x$ and *x* = *nh*, let the average slope over interval *h* be approximated by the average of the slopes at the beginning and the end of that interval.

$$\bar{F}'_n = \frac{F_n - F_{n-1}}{h} \approx \frac{1}{2}(F'_n + F'_{n-1}) = \frac{1}{2}\left[(1 - g'_n F_n) + (1 - g'_{n-1} F_{n-1})\right]. \tag{19}$$

Eq. (4) was used to evaluate expressions for the slopes on the right-hand side of Eq. (19). This implicit approach for generating the updated value F_n is known as the first order Adams-Moulton integration method, sometimes referred to as the trapezoidal rule. Solving for $F_n(x)$ for x as the nth interval of h:

$$F_n = \frac{2h}{2 + hg'_n} + F_{n-1}\left(\frac{2 - hg'_{n-1}}{2 + hg'_n}\right). \tag{20}$$

This form of quadrature provides better fidelity than the simpler backward Euler method for certain solutions such as the error function, which increasingly underpredicts at higher values of independent variable x.

Applications

The new function generator technique is applied to some existing integrals, where properties of functions associated with them, previously existing or not, are explored in original and transformed space.

Sievert Integral

The Sievert integral is used by radiologists to compute tissue radiation exposure rate from a thin, cylindrical implanted radiological source as a function of position:[5,6]

$$I(\phi, x) \equiv \int_0^{\phi} e^{-x\sec\phi} d\phi . \tag{21}$$

Comparing Eq. (21) with Eqns. (2-4), one finds

$$g(\phi) = -x\sec\phi; \quad g' = -x\tan\phi\sec\phi; \quad I = e^{-x\sec\phi}F(\phi, x); \quad \text{and} \quad F' - x\tan\phi\sec\phi\, F = 1. \tag{22}$$

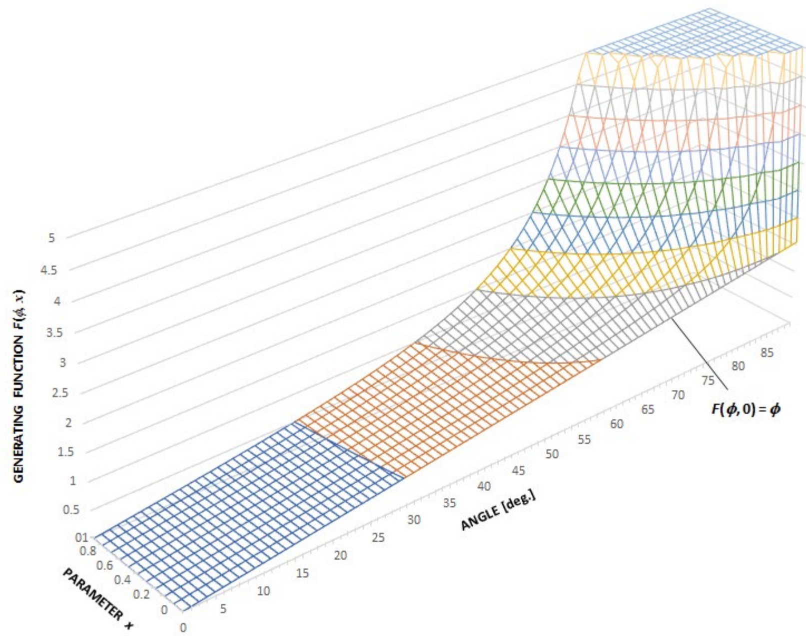

Figure 3. Three-dimensional contour map for $F(\phi, x)$ that solves the Sievert integral in transformed space.

The differential equation listed on the right-hand side of Eq. (22) uses angle ϕ as the integration variable, and x is a free parameter representing the product of source rod radius and intensity attenuation coefficient through the surrounding tissue.[5] In transformed space, quadrature for function F was performed using Eq. (20). Results are presented in Fig. 3. Notice in the limit of x = 0 that $F(\phi, 0) = \phi$, measured in radians. Solution to the integral is given by the function $I(\phi, x) = e^{-x \sec\phi} F(\phi, x)$. This result is depicted in Figs. 4 & 5, and values on the solution surface agree with values tabulated in Table 27.4 of Ref. 6.

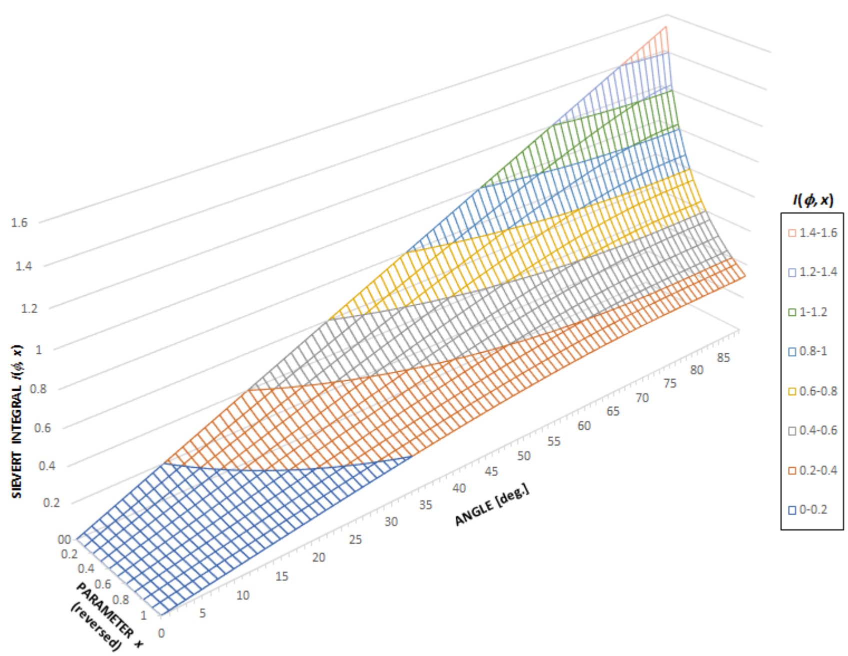

Figure 4. Contour map depicting the solution to the Sievert integral.

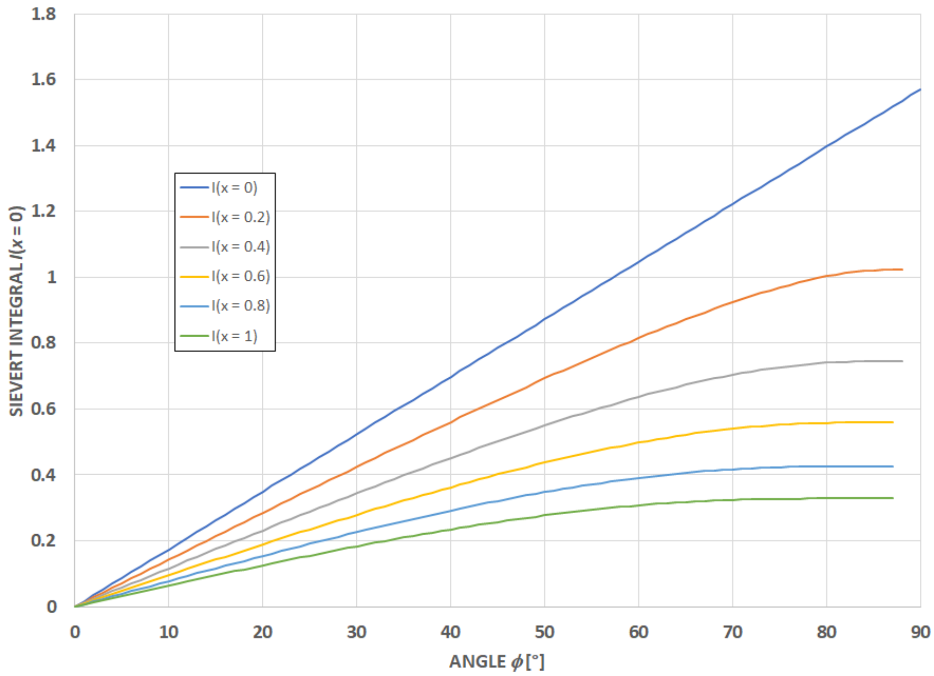

Figure 5. Sievert integral function for various *x*, $0 \leq x \leq 1$.

When converting from *F* to *I*, $I(\phi,0)=\phi$, and for $x > 0$ it produces relatively lower values than for $x = 0$ at a given positive angle. As *x* increases, $I(\phi,x)$ tends to asymptote to constant values as *f* increases. This observation may produce a useful approximation in practice since $\sec\phi \to \infty$ as $\phi \to \pi/2$. Due to this singularity and the physical interpretation of angle ϕ, no attempts were made to compute the solution for $\phi > \pi/2$.

Although it appears unnecessary to attempt creating an asymptotic expansion for this periodic function, generation of a Maclaurin series was pursued. Application of Eq. (16) to the differential equation described in Eq. (22) produces

$$F(\phi,x) = \phi + \frac{x}{3}\phi^3 + \frac{5x+2x^2}{30}\phi^5 + \ldots \tag{23}$$

and

$$I(\phi,x) = e^{g(\phi)}F(\phi,x) = e^{-x\sec\phi}\left(\phi + \frac{x}{3}\phi^3 + \frac{5x+2x^2}{30}\phi^5 + \ldots\right). \tag{24}$$

In Eqns. (23) & (24) and for other computations, angles are assumed to use units of radians, although it is convenient to plot using degrees instead. Figures 6 & 7 show results for the Sievert integral with $x = 0.5$ and $x = 5$, along with the Maclaurin series created from the first few terms listed in Eq. (24).

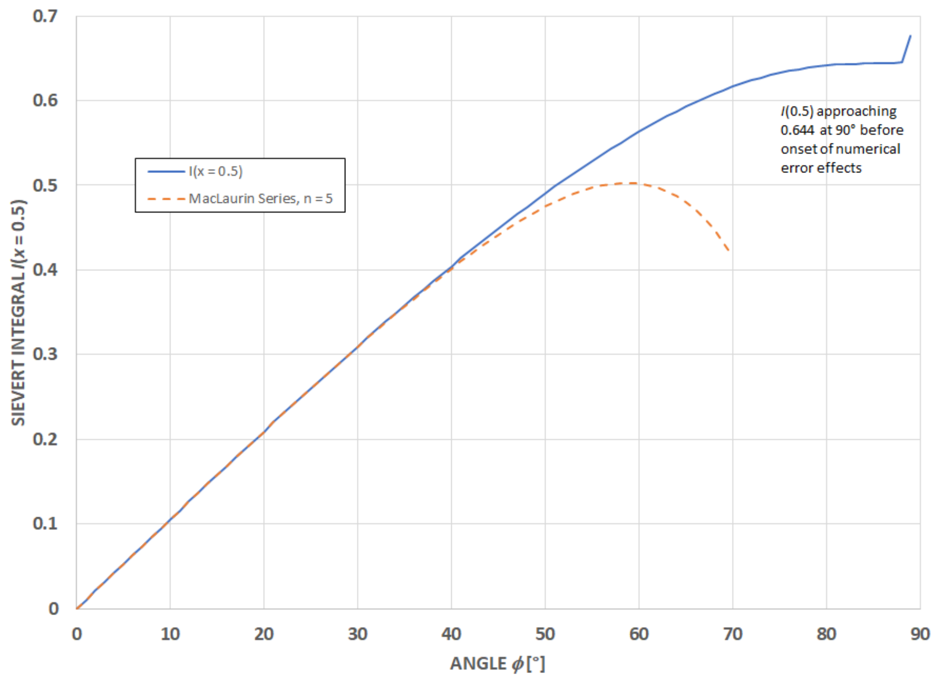

Figure 6. Sievert integral for x = 0.5 based on Eq. (22), along with Maclaurin series Eq. (24).

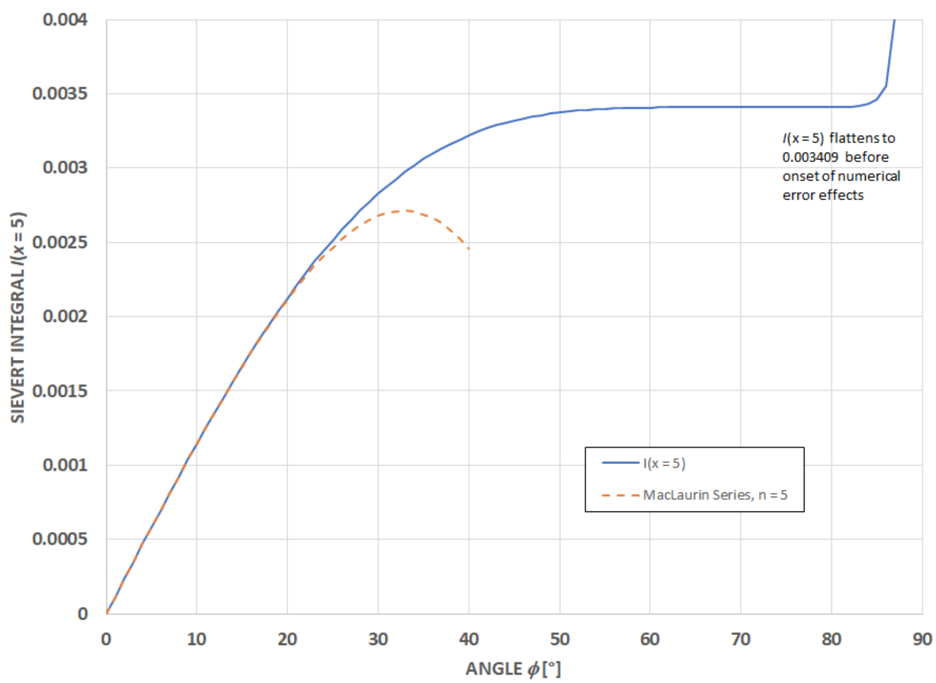

Figure 7. Sievert integral for x = 5 based on Eq. (22), along with Maclaurin series Eq. (24).

Modified Bessel Function of the First Kind, Order Zero

This integral arises in a number of physical situations, for instance in development of the scattering kernel for the Cercignani-Lampis gas surface interaction model.[7]

$$I_0(x) \equiv \frac{1}{\pi}\int_0^{\pi} e^{x\cos\theta} d\theta \,. \tag{25}$$

In technical literature, $I_0(x)$ is sometimes introduced using an alternative definition,[8]

$$I_0(x) \equiv \frac{1}{2\pi}\int_0^{2\pi} e^{x\cos\theta} d\theta \,. \tag{26}$$

Since this integral takes on a form that is readily transformed within the context of the function generator technique, it was decided to replace the upper integration limit with variable θ to create a function that may easily be transformed and also be relatable to either Eq. (25) or (26):

$$B(\theta, x) \equiv \int_0^{\theta} e^{x\cos\theta} d\theta \,. \tag{27}$$

This integral can be transformed directly to $F(\theta, x)$ with the following properties:

$$g(\theta) = x\cos\theta; \qquad g' = -x\sin\theta; \qquad B = e^{-x\sin\theta}F(\theta, x); \quad \text{and} \quad F' - x\sin\theta\, F = 1. \tag{28}$$

The differential equation for F in Eq. (28) was numerically integrated using the Adams-Moulton method to produce the contour maps depicted in Figs. 8 & 9. Although the function exhibits periodicity, it is not completely periodic, as its maxima and minima increase with angle as θ extends beyond 2π.

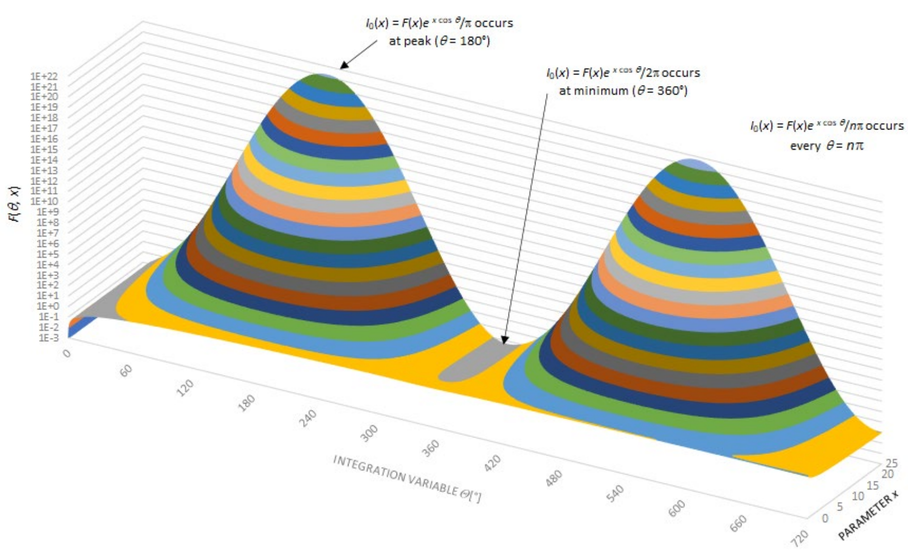

Figure 8. Three-dimensional contour map for $F(\theta, x)$ that solves the Modified Bessel Function of the First Kind, Order Zero in transformed space (logarithmic scale).[9]

Since $F(\theta, x)$ varies so tremendously with angle, it has been replotted using a linear scale in Fig. 9 to observe its behavior closer to zero. Once again in transformed space, a limiting relationship of $F(\theta, 0) = \theta$ is apparent.

The conversion was then inverted to compute $I_0(\theta, x)$ as some function of $B(\theta, x)$. Over the interval $\theta = [0, \pi]$, Eq. (27) was applied to Eq. (25) (see Fig. 10). A linear relationship was found for x = 0, with the correct result for $I_0(x)$ found at $\theta = \pi$, as expected from the upper integration limit in Eq. (25).

Comparing Eqns. (25) & (26), two approaches were chosen to determine whether the correct result for $I_0(x)$ would also appear at $\theta = 2\pi$ and perhaps every multiple of π thereafter. The first inversion approach was meant to show whether $I_0(x)$ could be computed at any angle θ by trying $I_0(\theta, x) = \theta B(\theta, x)$. Results are presented in Fig. 11. It was found that although $I_0(x)$ did not occur at every angle θ, it did occur for $\theta = n\pi$, where n is a positive integer. While one observes maxima occurring in the transformed function F for odd values of n and minima for even values, these correspond to non-extreme descending and ascending sections in $I_0(\theta, x)$, respectively.

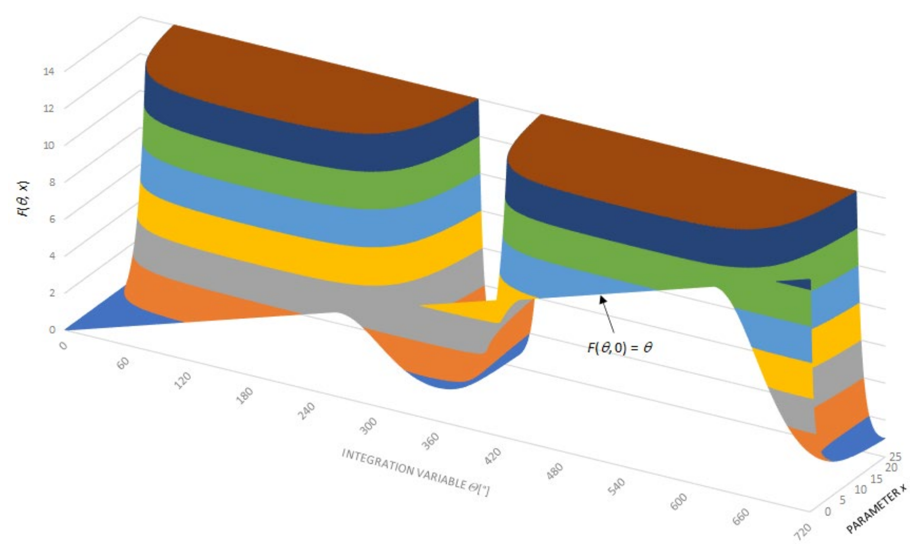

Figure 9. Linear scale close-up of $F(\theta, x)$ featuring linear relationship for x = 0.

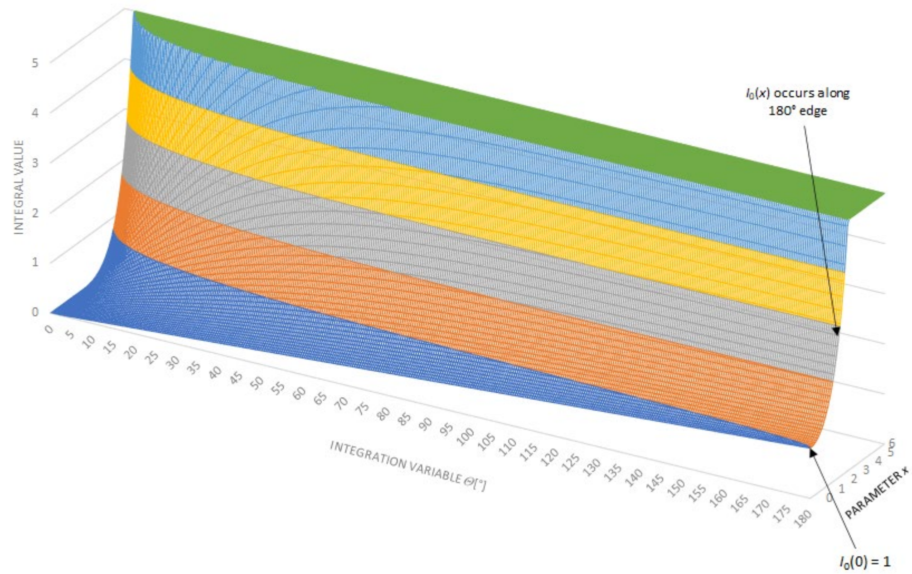

Figure 10. Linear scale close-up of $\pi B(\theta, x)$ featuring linear relationship for x = 0. Right-hand edge at $\theta = \pi$ produces $I_0(x)$.

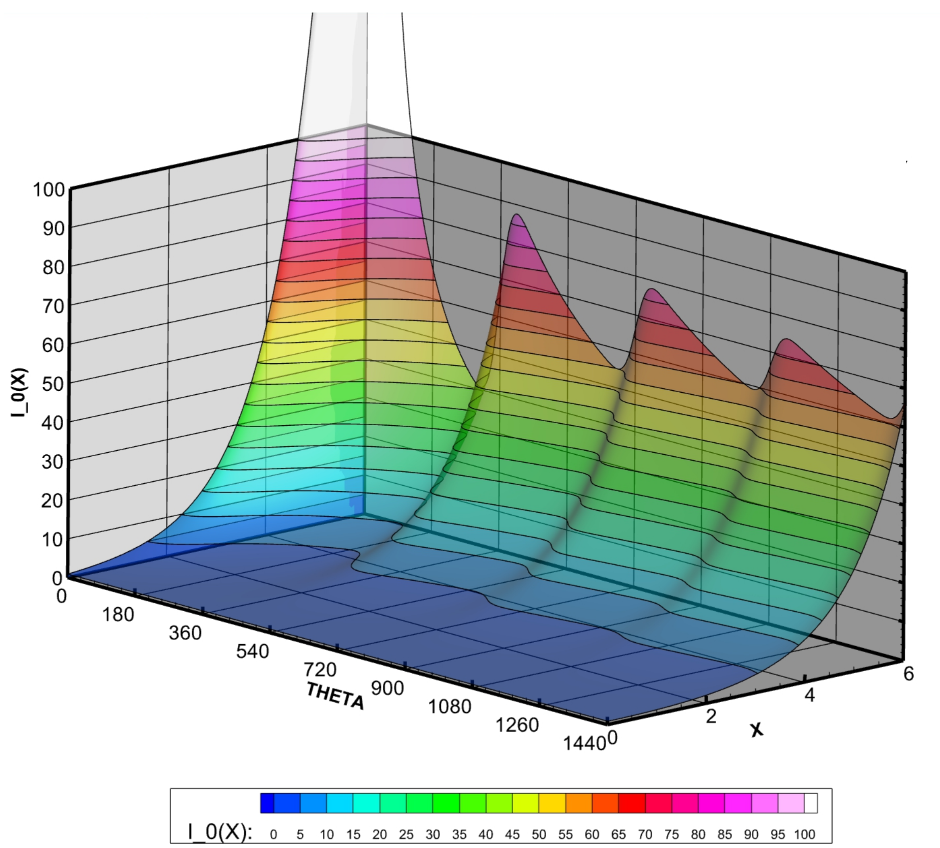

Figure 11. Inversion of F assuming $I_0 = \theta B$. Surface yields $I_0(x)$ every $\theta = n\pi$.

The second approach for inverting $F(\theta, x)$ to compute $I_0(\theta, x)$ from $B(\theta, x)$ involved renormalizing $B(\theta, x)$ by increasing factors of *p* in discrete intervals, such as π for $\theta = [0, \pi]$, 2π for $\theta = (\pi, 2\pi]$, $n\pi$ for $\theta = ((n-1)\pi, n\pi]$, *etc*. This approach was meant to observe whether differences in multiple definitions for $I_0(x)$ would continue for increasing angle.

Results are shown in Fig. 12 below. Not only is $I_0(x)$ present for every $\theta = n\pi$, but the contour map indicates how $I_0(x)$ is approached as a function of *q*. For intervals associated with odd values of *n*, $I_0(\theta, x)$ asymptotes rapidly to $I_0(x)$, while within intervals associated with even *n*, $I_0(\theta, x)$ idles at lower values, eventually ramping up to produce $I_0(x)$. Discontinuities are associated with transitions due to renormalization. There is a similar discontinuity in the neighborhood of $\theta \approx 0^+$ that may be due to assumptions made to start the numerical integration. It does not appear likely that $I_0(x)$ could be produced at $\theta = 0$ since the integration interval has zero width.

Interrogation of the solution surfaces depicted in Figs. 11 & 12 result in repetition of $I_0(x)$ for every $\theta = n\pi$ (Fig. 13).

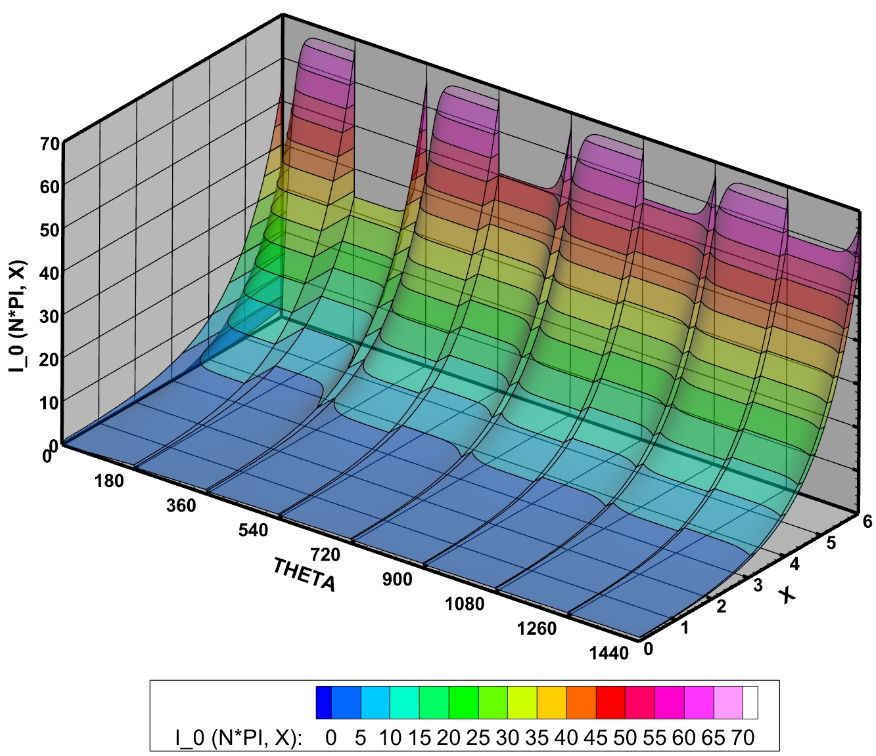

Figure 12. Inversion of *F* assuming $I_0 = n\pi B$ with renormalization in $\theta = n\pi$ increments. Surface produces $I_0(x)$ every $\theta = n\pi$.

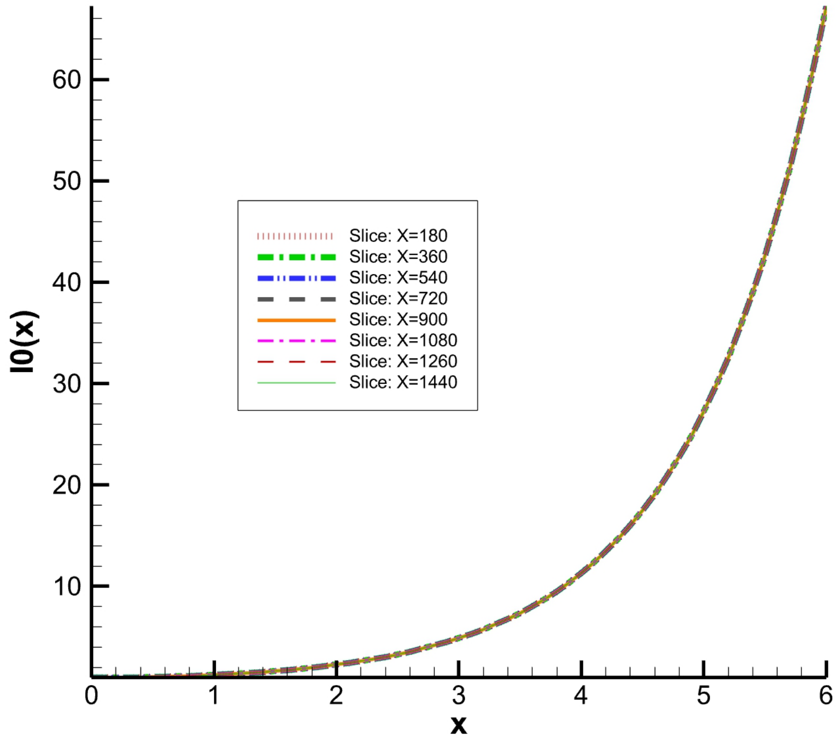

Figure 13. Values extracted from Fig. 11 or Fig. 12 every $\theta = n\pi$ correctly produce $I_0(x)$.

Since the function generator technique uses θ as its independent variable and not x, no asymptotic expansion or Maclaurin series was created in this investigation.

Error Function

The error function erf(x) is generated by the integrated area under the Gaussian distribution function and is very important for describing diffusion processes of heat conduction or trace molecular species in physical systems. It is usually defined in a normalized format:

$$\mathrm{erf}(x) \equiv \frac{2}{\sqrt{\pi}} \int_0^x e^{-x^2} dx . \tag{29}$$

For this function, important elements of the transformation process include

$$g(x) = -x^2; \qquad g' = -2x; \qquad \mathrm{erf}(x) = \frac{2}{\sqrt{\pi}} e^{-x^2} F(x); \quad \text{and} \quad F' - 2xF = 1. \tag{30}$$

One observes a certain similarity between the differential equation produced for erf(x) in Eq. (30) and that for the Dawson function discussed after Eq. (7) $(D' + 2xD = 1)$.

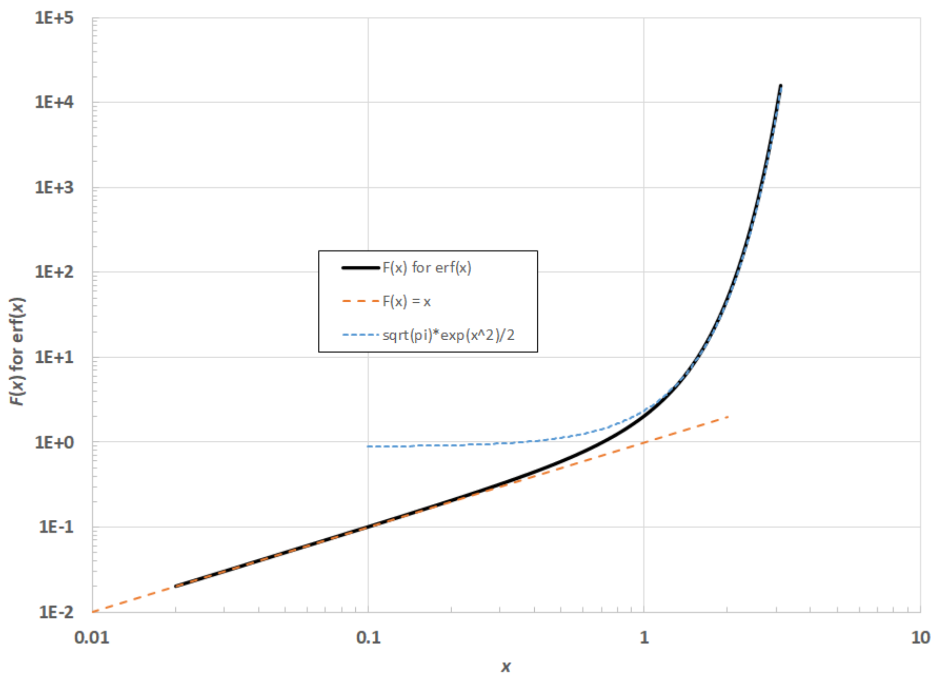

Figure 14. Transformed function $F(x)$ for erf(x) using the function generator technique.

This function contains only one variable, so the transformed function $F(x)$ is depicted on a two-dimensional plot in Fig. 14 using an integration step size $h = \Delta x = 0.01$. As often occurs in transformed space, $F(x) \approx x$ near $x = 0$. Also, recognizing that erf(x) approaches unity for large values of x, it is not surprising from Eq. (30) to observe that

$$F(x) \xrightarrow[x\to\infty]{} \frac{\sqrt{\pi}}{2} e^{x^2}. \tag{31}$$

Eq. (16) was used to produce terms of the Maclaurin series rising from x = 0 (Fig. 15). Different sets of correction terms are plotted along with the error function produced by the function generator technique using the Adams-Moulton numerical quadrature scheme on $F(x)$:

$$F(x) = x + \frac{2}{3}x^3 + \frac{4}{15}x^5 + \frac{8}{105}x^7 + \frac{16}{945}x^9 + \frac{32}{10395}x^{11} + \ldots = \sum_{n=0}^{\infty} \frac{2^n x^{2n+1}}{(2n+1)!!}, \tag{32}$$

and from Eq. (30),

$$\operatorname{erf}(x) = \frac{2}{\sqrt{\pi}} e^{-x^2} F(x). \tag{33}$$

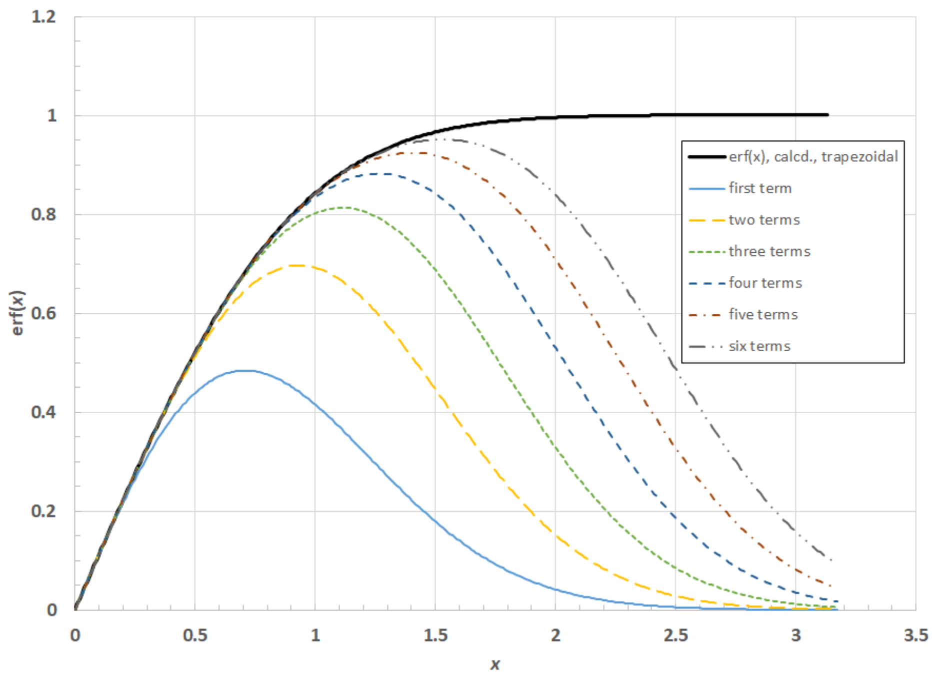

Figure 15. Error function erf(x) generated via function generator inversion of $F(x)$ along with successive terms of the Maclaurin series expansion.

The Maclaurin series computed here matches the expression presented in standard mathematical reference materials.[10] It is interesting to note that despite the fact that each term in the series is positive, the overall series does not appear to ever overshoot erf(x). Series featuring terms with alternating signs seemingly tend to straddle their functions (see Fig. 2).

The asymptotic expansion generated using this technique runs into problems. Use of Eqns. (5) & (6) lead to

$$F(x) \xrightarrow{?} -\frac{1}{2x}+\frac{1}{4x^3}-\frac{3}{8x^5}+\frac{15}{16x^7}-\ldots=\sum_{n=1}^{\infty}(-1)^n\frac{(2n-3)!!}{2^n x^{2n-1}}. \tag{34}$$

$$\text{"erf}(x)\text{"}=\frac{2}{\sqrt{\pi}}e^{-x^2}F(x) \xrightarrow{?} \frac{e^{-x^2}}{\sqrt{\pi}}\sum_{n=1}^{\infty}(-1)^n\frac{(2n-3)!!}{2^{n-1}x^{2n-1}} \sim -\frac{e^{-x^2}}{\sqrt{\pi}x}. \tag{35}$$

It is apparent that as $x \to \infty$, the series described by Eq. (35) will tend to zero, while it is already known that this function should converge to unity. It may happen that this large argument series expansion is affected by the discussion surrounding Eq. (9) and may need further special treatment. Notably in standard mathematical references, the asymptotic expansion for the complementary function erfc(x) is given by[10,11]

$$\text{erfc}(x) \xrightarrow[x\to\infty]{} \frac{e^{-x^2}}{\sqrt{\pi}x}\left\{1+\sum_{m=1}^{\infty}(-1)^m\frac{(2m-1)!!}{\left(2x^2\right)^m}\right\}. \tag{36}$$

Evaluation of Eq. (36) shows the asymptotic expansion developed by the function generator approach−Eq. (35)−errs in a way that actually describes $-\text{erfc}(x)=\text{erf}(x)-\text{erf}(\infty)$ instead!

Lower Incomplete Gamma Function

The lower incomplete gamma function $\gamma(s,x)$ has been encountered when analyzing rigid vessel venting under certain forcing conditions. It is described by the integral producing gamma function $\Gamma(s)$, but with the upper integration limit reduced from ∞ to some finite value *x*:[12,13]

$$\gamma(s,x) \equiv \int_0^x t^{s-1} e^{-t} dt. \quad (37)$$

Using the variable substitution $z \equiv t^s$ or x^s, one finds

$$s\,\gamma(s,x) = I(s,z) \equiv \int_0^z e^{-z^{\frac{1}{s}}} dz; \quad \text{where} \quad x = z^{\frac{1}{s}}. \quad (38)$$

Notice that with this variable change, the integral and the variable for the transformed function is *z*, while the original function uses *x*, so this extra step will need to be accounted for when inverting *F*(*z*).

One notes the error function erf(*x*) is itself a special case of Eq. (38).[13] When $s = 1/2$,

$$\gamma\left(\frac{1}{2},x\right) = 2\int_0^{z=\sqrt{x}} e^{-z^2} dz = \sqrt{\pi}\,\text{erf}\left(\sqrt{x}\right). \quad (39)$$

Working with integral *I*(*s*, *z*), here are important elements of the transformation process:

$$g(z) = -z^{\frac{1}{s}}; \qquad g' = -\frac{1}{s} z^{\frac{1-s}{s}}; \qquad I(s,z) = e^{-z^{\frac{1}{s}}} F(s,z); \quad \text{and} \quad F' - \frac{1}{s} z^{\frac{1-s}{s}} F = 1. \quad (40)$$

In Eq. (40), differentials are taken with respect to integration variable *z*, and *s* is an independent variable parameter. The differential equation was integrated and plotted as a contour map in Fig. 16 below using $h = \Delta z = 10^{-3}$. A cut across this surface at $s = 1/2$ produces a curve proportional to Fig. 14 for the error function (with $\sqrt{x}$ as its argument).

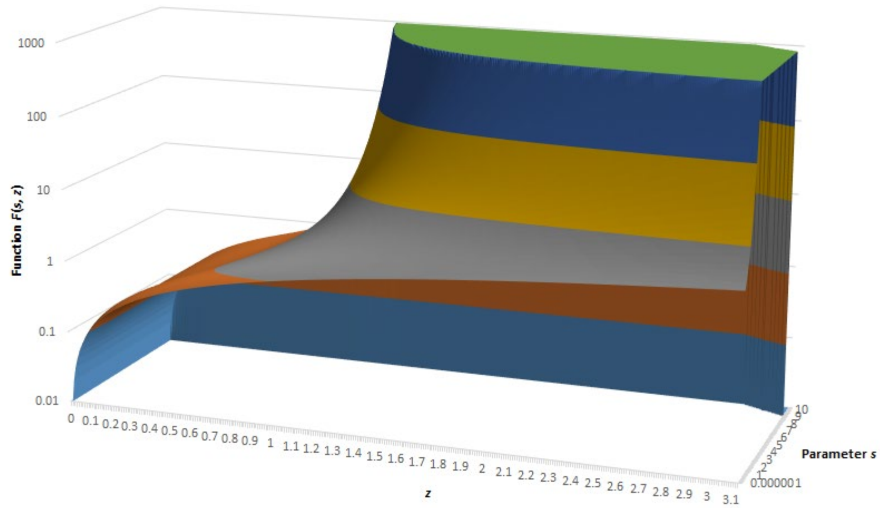

Figure 16. Contour map for transformed function $F(s, z)$ that solves Eq. (37).

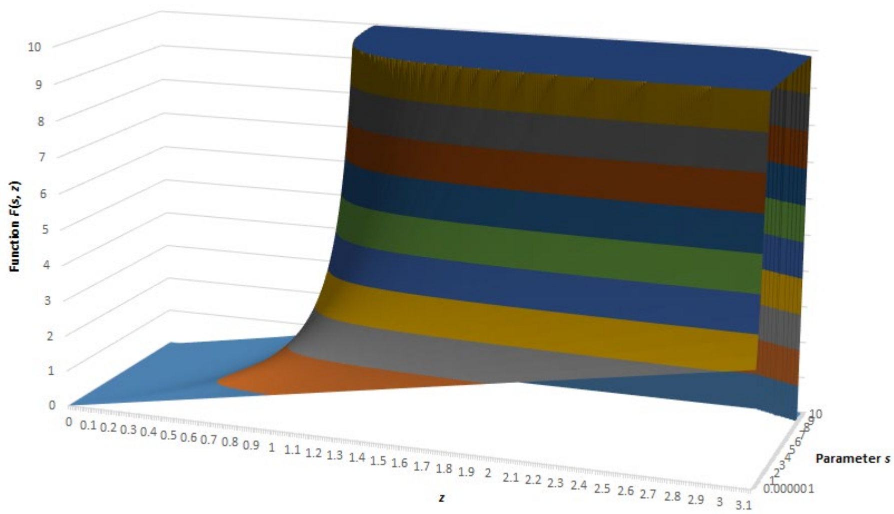

Figure 17. Linear scale detail for $F(s, z)$ featuring linear relationship for $s = 0$.

Since $F(s, z)$ varies so tremendously and rapidly becomes unbounded, it has been replotted with a focus on values closer to zero on a linear scale (Fig. 17). Note the linear relationship $F(0, z) = z$ where $s = 0$, as well as the steepness of the contour map rising from low values of either s or z.

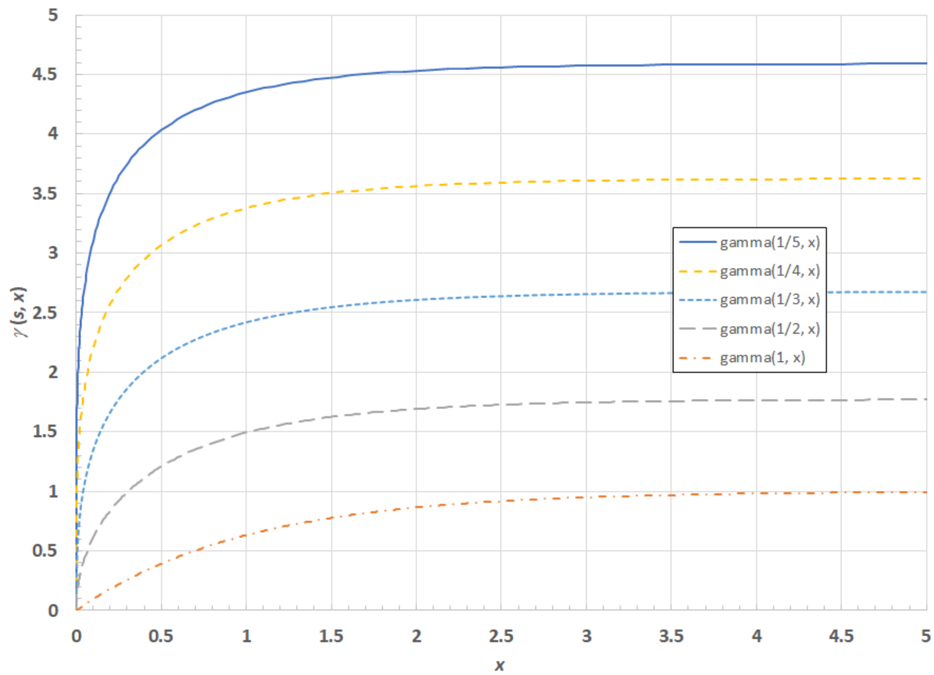

Figure 18. Lower incomplete gamma function $\gamma(s,x)$ for various values of s, inverted and converted from $F(s, z)$.

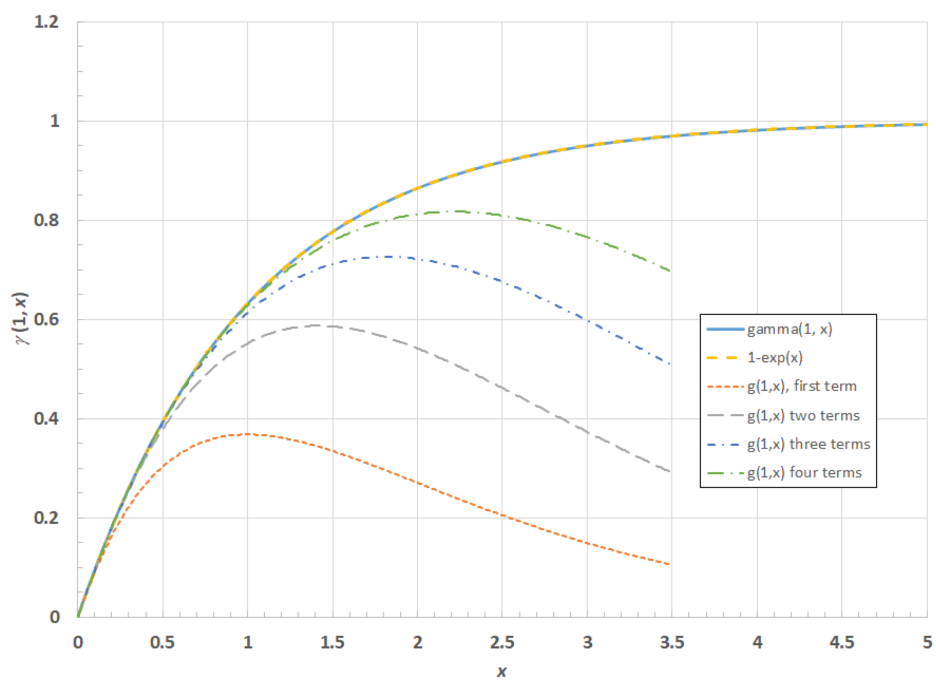

Figure 19. Lower incomplete gamma function $\gamma(1,x)$, inverted and converted from $F(s, z)$, plotted along with successive terms of the Maclaurin series expansion.

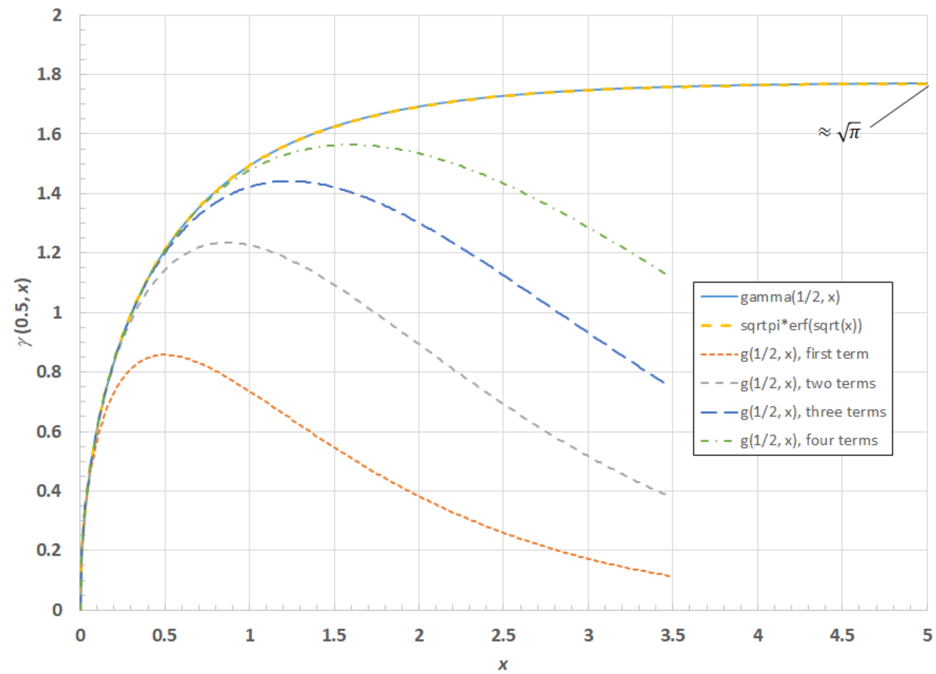

Figure 20. Lower incomplete gamma function $\gamma(1/2, x)$, inverted and converted from *F*(*s*, *z*). Results compared to Eq. (39) relationship with error function. Successive terms of the Maclaurin series expansion are also included.

Figures 18-20 present results for the lower incomplete gamma function as a function of *x* inverted from *F*(*s*, *z*) for various values of *s* where 1/*s* is an integer. As *s* becomes smaller, the curves become increasingly bluff, reaching higher asymptotes at lower values of *x*.

It was not possible to create Maclaurin series for $\gamma(s,x)$ from the function generator technique except when *s* takes on values of inverse integers. This becomes evident when evaluating *F*(*s*, *z*) using Eqn. (16) or its equivalent because higher derivatives of $\gamma(s,z)$ generally will eventually generate inverse powers of *z*. Once this happens, a singularity arises when evaluating at *z* = 0. The only exceptions occur when inverse values of *s* are integers. Let $m \equiv 1/s$. Depending on the value of *s*, only every m^{th} term is non-zero after the linear factor.

$$F(1,z) = \sum_{n=0}^{\infty} \frac{F^{(n)}(1,0)}{n!} z^n = \sum_{n=0}^{\infty} \frac{z^n}{n!} = e^z;$$

$$F\left(\frac{1}{2},z\right) = z + \frac{2\times 2!}{3!}z^3 + \frac{4\times 2!\times 2\times 2!}{5!}z^5 + \frac{6\times 2!\times 4\times 2!\times 2\times 2!}{7!}z^7 + \ldots = \sum_{n=1}^{\infty}(2n-2)!!\frac{(m!)^{n-1} z^{2n-1}}{(2n-1)!};$$

$$F\left(\frac{1}{3},z\right) = z + \frac{3\times 3!}{4!}z^4 + \frac{15\times 3!\times 3\times 3!}{7!}z^7 + \ldots = \sum_{n=1}^{\infty} \frac{(m!)^{n-1} z^{3n-2}}{(3n-2)!} \prod_{k=0}^{n-1} \binom{3k}{2}. \tag{41}$$

In general,

$$F(m,z) = \sum_{n=1}^{\infty} \frac{(m!)^{n-1} z^{m(n-1)+1}}{[m(n-1)+1]!} \prod_{k=0}^{n-1} \binom{km}{m-1}. \tag{42}$$

The binomial coefficients in Eq. (42) may be found by constructing Pascal's triangle in straightforward fashion. The resulting Maclaurin series for $\gamma(s,x)$ where $z = x^s$ for those special cases of integer m = 1/s become

$$\gamma(s,x) = me^{-x}\sum_{n=1}^{\infty}\frac{(m!)^{n-1}z^{m(n-1)+1}}{[m(n-1)+1]!}\prod_{k=0}^{n-1}\binom{km}{m-1}. \tag{43}$$

Sets of the first few terms of the Maclaurin series for m = 1 & 2 cases have been added to Figs. 19 & 20, respectively.

Once again, the asymptotic expansion for $x \to \infty$ created by this function generator approach runs into problems. Application of Eqns. (5) & (6) produces

$$\frac{1}{g'} = -sz^{1-\frac{1}{s}};\quad \frac{1}{g'}\left(\frac{1}{g'}\right)' = s(s-1)z^{1-\frac{2}{s}};\quad \frac{1}{g'}\left(\frac{1}{g'}\left(\frac{1}{g'}\right)'\right)' = -s(s-1)(s-2)z^{1-\frac{3}{s}};\ldots. \tag{44}$$

For the product factors being produced, perhaps it is useful to restrict this development to $s > 1$, which is a different region for which Maclaurin series were generated. Eq. (44) terms combine to produce

$$F(s,z)\xrightarrow{?}-\sum_{n=1}^{n<s}\frac{s!z^{1-\frac{n}{s}}}{(s-n)!};\qquad s>1, \tag{45}$$

and

$$"\gamma(s,x)"\xrightarrow{?}-\frac{e^{-x}}{s}\sum_{n=1}^{n<s}\frac{s!x^{s-n}}{(s-n)!} = -e^{-x}(s-1)!\sum_{n=1}^{n<s}\frac{x^{s-n}}{(s-n)!};\qquad s>1. \tag{46}$$

If s is a positive integer, then

$$"\gamma(s,x)"\xrightarrow{?}-e^{-x}(s-1)!\sum_{k=0}^{s-1}\frac{x^k}{k!} = -e^{-x}(s-1)!\,e_{s-1}(x). \tag{47}$$

The summation in Eq. (47) is recognized as the truncated Maclaurin series for the exponential function e^x after an integer number of $s-1$ terms, which is defined as the exponential sum function.

In actuality, $\gamma(s,x)$ and its complementary upper incomplete gamma function $\Gamma(s,x)$ combine to produce the (complete) gamma function $\Gamma(s)$, which is like $\gamma(s,\infty)$. The asymptotic expansion for upper incomplete gamma function $\Gamma(s,x)$ for integer s is[12]

$$\Gamma(s,x)\xrightarrow[x\to\infty]{}e^{-x}(s-1)!\,e_{s-1}(x). \tag{48}$$

So it appears that Eq. (47) has erred in the sense that in actually computing $-\Gamma(s,x) = \gamma(s,x)-\Gamma(s)$, or $\gamma(s,x)-\gamma(s,\infty)$. Along these lines one is reminded the expression Eq. (35) computed for the asymptotic expression of the error function is actually erf(x) – erf(∞).

Reviewing the behavior of these asymptotic expansions, it is possible that when corrected by $\Gamma(s)$, a general form for $\gamma(s,x)$ without specifying s as an integer becomes

$$\gamma(s,x)\xrightarrow[x\to\infty]{?}\Gamma(s)\left\{1-e^{-x}\sum_{n=1}^{n<s}\frac{x^{s-n}}{\Gamma(s-n+1)}\right\}. \tag{49}$$

Concluding Remarks

General properties associated with functions created by this function generator scheme have been presented in greater detail than before. Further developments include formulation of a generalized Maclaurin series and presentation of a powerful, simple numerical quadrature scheme geared to produce values of functions generated using this technique. Certain limitations associated with application of this technique to Maclaurin series and asymptotic expansions are also discussed.

The function generator technique was used to describe solutions for integrals that have already been studied for comparison purposes. Even so, limitations to the technique's formulations for asymptotic expansions exhibit correct behavior to within constant values for the error function and lower incomplete gamma functions. The nature of this scheme's deficiency appears to suggest a correction leading to a generalized format for $\gamma(s,x)$.

In addition, the technique produced a new function that solves the Sievert integral and gives that function's Maclaurin series, as well as a new function associated with the modified Bessel function of the first kind, order zero that exhibits a form of periodicity relating multiple definitions of that particular function over different periods to one another.

References

[1] Woronowicz, M., "New Mathematical Functions for Vacuum System Analysis," *NASA/CR-2017-219017*, January 2017.

[2] Woronowicz, M., "Some General Properties for a Newly Discovered Class of Mathematical Functions," *NASA/CR-2018-219028*, April 2018.

[3] *Handbook of Mathematical Functions With Formulas, Graphs, and Mathematical Tables*, eds. M. Abramowitz and I. Stegun, National Bureau of Standards, Applied Mathematics Series 55, Washington, DC, June 1964, pp. 297-319.

[4] Oldham, K., *et al*., *An Atlas of Functions*, 2nd ed., Springer Science+Business Media, LLC, New York, 2009, pp. 427-33.

[5] Williamson, J., *et al*, "Monte Carlo evaluation of the Sievert integral for brachytherapy dosimetry," *Physics in Medicine & Biology*, Vol. 28, 1983, pp. 1021-1033.

[6] *Handbook of Mathematical Functions With Formulas, Graphs, and Mathematical Tables*, eds. M. Abramowitz and I. Stegun, National Bureau of Standards, Applied Mathematics Series 55, Washington, DC, June 1964, pp. 1000-1001.

[7] Cercignani, C., and Lampis, M., "Free Molecular Flow Past a Flat Plate in the Presence of a Nontrivial Gas-Surface Interaction," *Journal of Applied Mathematics and Physics (Zeitschrift für Angewandte Mathematik und Physik)*, Vol. 23, Dec. 1972, pp. 713-728.

[8] Sharipov, F., and Seleznev, V., "Data on Internal Rarefied Gas Flows," *Journal of Physical and Chemical Reference Data*, Vol. 27, 657, 1998, pp. 657-706.

[9] Geisel, T., *Oh the Places You'll Go!* Random House, 1990.

[10] *Handbook of Mathematical Functions With Formulas, Graphs, and Mathematical Tables*, eds. M. Abramowitz and I. Stegun, National Bureau of Standards, Applied Mathematics Series 55, Washington, DC, June 1964, pp. 297-300.

[11] Oldham, K., *et al*., *An Atlas of Functions*, 2nd ed., Springer Science+Business Media, LLC, New York, 2009, pp. 408-409.

[12] Temme, N., "Computational Aspects of Incomplete Gamma Functions with Large Complex Parameters," in *Approximation and Computation: A Festschrift in Honor of Walter Gautschi*, *International Series of Numerical Mathematics, Vol. 119,* ed. R. Zahar, Birkhäuser, Boston, 1994, pp. 551-562.

[13] Gautschi, W., "The Incomplete Gamma Functions Since Tricomi," in *Tricomi's Ideas and Contemporary Applied Mathematics*, *Atti dei Convegni Lincei*, *n. 147*, Accademia Nazionale dei Lincei, 1998, pp. 203-237.